Experimental Simulation of Titan's Stratospheric Photochemistry: Benzene (C 6 H 6) Ices

J. Mouzay, I. Couturier-tamburelli, N. Piétri, T. Chiavassa

JGR Planets

RESEARCH ARTICLE
10.1029/2020JE006566

Experimental Simulation of Titan's Stratospheric Photochemistry: Benzene (C_6H_6) Ices

J. Mouzay[1], I. Couturier-Tamburelli[1], N. Piétri[1], and T. Chiavassa[1]

[1]Aix-Marseille Université, CNRS, PIIM, Marseille, France

Key Points:

- Laboratory experiments demonstrate that the interaction between FUV photons and benzene ice leads to a solid-state photochemical activity
- The in situ monitoring by infrared spectroscopy of the benzene ice photolysis leads to identify the formation of one of benzene's isomer, fulvene
- The photo-produced residue presents some IR features similar to those of Titan's aerosols probed by Cassini/VIMS

Supporting Information:

- Supporting Information S1

Correspondence to:
I. Couturier-Tamburelli,
isabelle.couturier@univ-amu.fr

Citation:
Mouzay, J., Couturier-Tamburelli, I., Piétri, N., & Chiavassa, T. (2021). Experimental simulation of Titan's stratospheric photochemistry: Benzene (C_6H_6) ices. *Journal of Geophysical Research: Planets*, *126*, e2020JE006566. https://doi.org/10.1029/2020JE006566

Received 12 JUN 2020
Accepted 22 DEC 2020

Author Contributions:
Formal analysis: J. Mouzay
Funding acquisition: I. Couturier-Tamburelli
Supervision: I. Couturier-Tamburelli, N. Piétri
Writing – original draft: J. Mouzay, I. Couturier-Tamburelli
Writing – review & editing: I. Couturier-Tamburelli, N. Piétri, T. Chiavassa

Abstract We performed laboratory experiments to study the photochemical evolution induced by long-UV irradiation of benzene ices in Titan's atmosphere. The aim of this study was to investigate whether photo-processed benzene ices could lead to the formation of aerosols analogs to those observed in Titan's stratosphere. Prior to that, spectroscopic properties of amorphous and crystalline benzene ices were studied as a function of temperature, using infrared spectroscopy. UV photolysis experiments ($\lambda > 230$ nm) of benzene ices led to the formation of volatile photo-products, among which fulvene is identified, and of a residue dominated by νCH IR features, demonstrating that pure aromatic-based polymeric structures are not sufficient to explain the composition of Titan's stratospheric haze layer. However, we provide a characterization of long-UV-induced benzene-containing aerosol analogs, which will contribute to Titan's surface organics layer. These data are of prime interest in the context of the future Dragonfly space mission.

Plain Language Summary Titan, often compared with the early Earth, is the only moon in the solar system to have a dense atmosphere, mainly composed of nitrogen and methane. In the upper part of the atmosphere (>1,000 km), UV photons, photoelectrons, energetic ions and magnetospheric electrons induce the dissociation and the ionization of nitrogen and methane. These reactions lead to the formation of complex organic molecules—including hydrocarbons such as benzene—and aerosols in the high atmosphere (an organic haze responsible for Titan's brownish color), which are subject to different UV radiation classes depending on the altitude. Therefore, during their sedimentation toward the surface, these organic photoproducts are expected to be modified. Once the tropopause is reached, molecules like benzene (C_6H_6) condense and could evolve under FUV radiations ($\lambda > 200$ nm) and contribute to aerosol formation.

1. Introduction

Until its conclusion in September 2017, the Cassini-Huygens space mission permitted an extensive exploration of the atmosphere of Saturn's largest moon, Titan, and provided much information on its chemical composition (Coustenis et al., 2010; Hörst, 2017; Vinatier et al., 2010, and references therein). However, lots of data related to Titan's haze still remains to be analyzed, in particular the spectroscopic data which give evidence of its chemical composition complexity. The interpretation of data coming from Cassini, Voyager and ground-based observations has nevertheless provided evidence of hundreds of complex organic compounds such as hydrocarbons [ethane (C_2H_6), acetylene (C_2H_2), ethylene (C_2H_4), methylacetylene (C_3H_4), propane (C_3H_8), propene (C_3H_6), diacetylene (C_4H_2)], nitriles [hydrogen cyanide (HCN), cyanoacetylene (HC_3N), ethylcyanide (C_3H_5N), vinyl cyanide (C_3H_5N), and cyanogen (C_2N_2)] (Cordiner et al., 2015; Coustenis et al., 2007; Hanel et al., 1981; Kunde et al., 1981; Nixon et al., 2013; Palmer et al., 2017) and, as end products, aerosols which form haze layers (Hörst, 2017; Wilson & Atreya, 2003) in the atmosphere. All these organic particulates/molecules are produced by the dissociation and ionization of the main atmospheric constituents, N_2 and CH_4 (Lavvas et al., 2013; Liang et al., 2007; Waite et al., 2007). Based on their photochemistry, theoretical models predict the formation of simple molecules and of benzene, one of the most complex molecules observed to date (Krasnopolsky, 2014; Vuitton et al., 2006; Wilson & Atreya, 2003; Yung et al., 1984).

Detected for the first time by ISO (Coustenis et al., 2003), the presence of benzene vapor in Titan's atmosphere was confirmed by the Cassini Composite Infrared Spectrometer (CIRS) and the Cassini Ion and Neu-

tral Mass Spectrometer (INMS) (Waite et al., 2005) during the Cassini mission (Coustenis et al., 2007, 2003; Waite et al., 2007). Remote sensing measurements performed over a range of altitudes allowed the determination of the benzene mixing ratio (Coustenis et al., 2007; Cui et al., 2009; Koskinen et al., 2011). It decreases with altitude, indicating a high altitude production and a low altitude sink (Vuitton et al., 2008; Waite et al., 2007; Wilson & Atreya, 2004; Yoon et al., 2014) which is partially explained by a condensation process, as this is the main loss process of organics in Titan's atmosphere (Anderson et al., 2018, 2016; De Kok et al., 2007; Griffith et al., 2006; Khanna et al., 1987; Lavvas et al., 2011; Mayo & Samuelson, 2005; Samuelson & Mayo, 1991; Samuelson et al., 1997, 2007). Indeed, vapor condensation of organics occurs in the lower part of the stratosphere, where the temperature diminishes, at an altitude which depends, for a given compound, on several parameters such as its saturation vapor pressure, abundance and the local temperature, resulting in the formation of microscopic icy particles or aerosols (Lavvas et al., 2010, 2011). Using cloud microphysics and radiative transfer models, different groups (Barth, 2017; Lavvas et al., 2011) have published the condensation profile and cloud formation of the different gaseous species present in the stratosphere. They both proposed the condensation of benzene at around 85 km for temperatures of about 130 K from their models, based on the temperature profile measured during the descent of Huygens in the atmosphere (Fulchignoni et al., 2005) and vapor abundances measured at northern latitudes (Coustenis et al., 2010; Vinatier et al., 2015). However, seasonal dynamics can have an impact on ice formation, for instance during vertical dramatic cooling episodes, like the one that occurred at the south pole simultaneously to the reversal of Titan's atmospheric circulation, two years after the northern spring equinox (Bampasidis et al., 2012; Coustenis et al., 2016; Teanby et al., 2012). It resulted in an increase of the southern mixing ratios of benzene and other species (Coustenis et al., 2016, 2018). Near the south pole during the fall season in this hemisphere, Vinatier et al. (2018) detected benzene ice between high (~300 km, which is around three/four times higher than its expected condensation altitude) and low (<100 km) stratospheric altitudes.

Benzene is a particularly important molecule because it is suspected to play a key role in the formation of polycyclic aromatic hydrocarbons (PAHs), polyphenyls or polycyclic aromatic heterocycles (PANHs) or even aerosols at high altitude (e.g., Delitsky & McKay, 2010; Gautier et al., 2017; Lebonnois, 2002; Mahjoub et al., 2016; Waite et al., 2007). In fact, Vuitton et al. (2008) have suggested that benzene is formed in the highest atmospheric layers (>900 km) by ion molecule reactions and diffuses downward where it induces—under photolysis—the formation of phenyl radicals ($C_6H_5^{\bullet}$) known to be at the origin of a rich production of aromatics. A recent study has upgraded the benzene photochemical reaction network, highlighting the importance of neutral and ion reactions for the production of aromatic species such as toluene ($C_6H_5CH_3$) or ethylbenzene ($C_6H_5C_2H_5$) (Loison et al., 2019). In addition, some studies have been performed to investigate the influence of C_6H_6 in Titan's aerosol production, either theoretically (Delitsky & McKay, 2010; Lavvas et al., 2011; Lebonnois, 2005) or experimentally (Gautier et al., 2017; Sciamma-O'Brien et al., 2014, 2017; Sebree et al., 2014; Trainer et al., 2013; Yoon et al., 2014) by the incorporation of benzene into a N_2/CH_4 mixture using plasma discharges or far-UV radiations. However, to our knowledge, the role of gas phase benzene photolysis in Titan's atmosphere is well investigated while the role of benzene ice photolysis in the stratospheric production of aerosol particles has not yet been investigated experimentally (cf. Figure 1, Yoon et al., 2014). Previous experiments were performed under conditions (temperatures between 4 K and 19 K)/energy sources) relevant for the ISM, either to understate its fate under UV radiations (Rahul et al., 2020; Ruiterkamp et al., 2005) or ion bombardment (Callahan et al., 2013; Strazzulla & Baratta, 1991), or to identify its photo-degradation pathways with the help of matrix-isolated environment (Johnstone & Sodeau, 1991; Ruiterkamp et al., 2005). But none of these studies can be used as a reference for simulating Titan's low stratospheric environment. Previous experimental work conducted by Couturier-Tamburelli et al., 2018; Gudipati et al., 2013) focused on understanding FUV solar photon-induced aging process of nitrile ices formed under stratospheric-like conditions in the laboratory. The authors demonstrated the formation of polymeric residues after warming up irradiated ices whose infrared features correspond, for the most part, to those observed by the CIRS and VIMS (Visible and Infrared Mapping Spectrometer) instruments in the aerosol layer present in the stratosphere of Titan. Although recent experimental works focused on the fate of acetylene (Abplanalp et al., 2019) or N_2/CH_4 ices (Vasconcelos et al., 2020), no study has been performed on the fate of benzene ices at such stratospher-

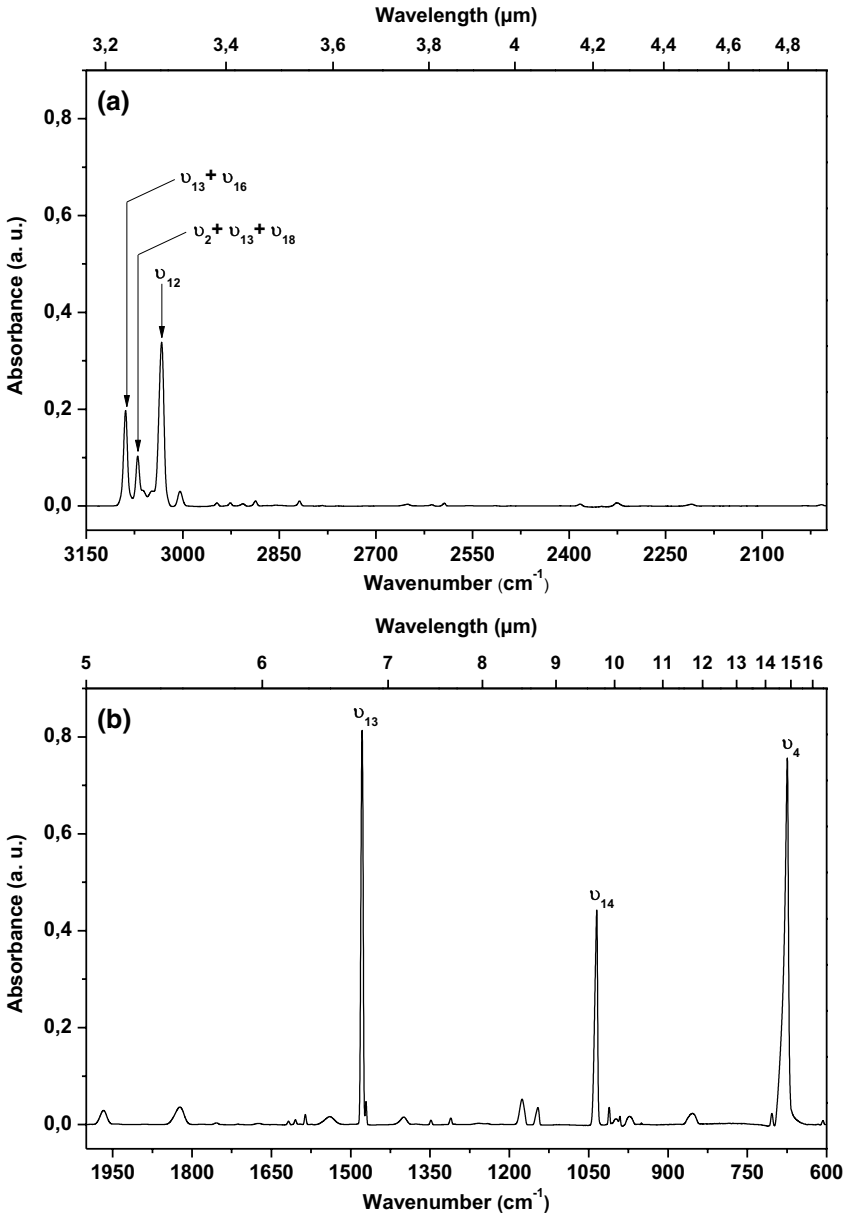

Figure 1. Infrared spectrum of amorphous benzene (deposited 16 K) in two regions: (a) between 3,150 and 2,025 cm^{-1} and (b) between 1,975 and 600 cm^{-1}; small bands on the spectrum correspond to harmonics or combination modes.

ic altitudes. As benzene is expected to condense below 100 km, that is, at altitudes mainly impacted by solar UV photons $\lambda > 230$ nm (Gudipati et al., 2013; Lavvas et al., 2008; Wilson, 2004), understanding the evolution of pure benzene ices submitted to low-energy photons is essential in identifying its subsequent contribution to the formation of aerosols that will participate in the organic layer that covers Titan's surface. Therefore, in this study, we conducted laboratory experiments to perform the photolysis of pure benzene ices, with photons at $\lambda > 230$ nm, in order to help in understanding the composition of photo-produced aerosols in the stratosphere. In particular, we highlight the role of benzene ice photolysis in the production of stratospheric aerosols by comparing our spectroscopic data with those of the stratospheric aerosol layer acquired by the VIMS instrument, before the period of formation of benzene ices at high altitude following the spring equinox.

2. Experimental Details

Benzene (for HPLC, assay ≥ 99.9%, from Sigma-Aldrich) was used after purification by vacuum distillation in several freeze-pump-thaw steps with the help of several liquid nitrogen baths. The absence of impurities (H_2O, CO_2) in each deposited benzene ice film was confirmed by IR spectroscopy. Benzene was deposited from a glass line onto a gold-plated surface located within a high vacuum chamber. The vacuum chamber pressure was 10^{-9} mbar for deposition temperature below 20 and 10^{-8} mbar for higher temperatures. The sample holder temperature was controlled from 16 to 300 K with a closed-cycle helium refrigerator and maintained using a model 21 CTI cold head cryostat, a resistive heater and a Lakeshore 331 temperature controller. Each deposited ice sample corresponded to a quantity of about 20 μmol of benzene. The quantity of sample deposited was chosen to obtain an intensity inferior to 1 a. u. on the IR spectra recorded. Samples were warmed up with a heating rate between 0.5 and 2 K.min^{-1}, this warm-up at 300 K resulted in a residue. IR spectra were recorded in reflection-absorption mode in the mid-infrared region between 4,000 and 4,600 cm^{-1} using a Bruker Tensor 27 Fourier transform infrared spectrometer with DTGS detector (Butscher et al., 2015). They were taken after deposition, after pumping the vacuum chamber back to base pressure, that is, without benzene vapor flowing in the chamber, and after rotating the sample holder. Each spectrum was averaged over 100 scans during the photolysis experiment and over 500 scans for the vibrational analysis of the residue, with a resolution of 1 cm^{-1}, except for the background which was averaged over 300 scans with the same resolution. After deposition, the vacuum chamber was brought back to base pressure (10^{-9} mbar) before conducting photolysis experiments.

Photolysis experiments were performed using an Oriel 500 W high-pressure mercury lamp (λ = 200–2,500 nm) with discrete Hg lines in the UV-Vis region between 200 and 600 nm, where most of the photon flux of 2.34×10^{16} photon.cm^{-2}.s^{-1} (~13 mW.cm^{-2}) resides. The photolysis time (48 h) was chosen to simulate a period of time in which benzene ices can sediment in the stratosphere (here, considering a solar flux of ~10^{14} photons.cm^{-2}.s^{-1} at 100 km on Titan, the photons flux of the UV source employed is therefore 234 times more important than the one that reaches Titan's lower stratosphere. Two days of photolysis in laboratory corresponds to 468 days or 1.3 years on Titan. However, considering Titan's exposure to the sun during the day and night, these 1.3 years becomes 2.6 years). Besides, the sedimentation time scale of a particle in the stratosphere depends on several parameters such as the particle radius or the pressure and the altitude (e.g., Barth & Toon, 2003), Figure 5 shows the fall velocities depending on particle size). In addition, two supplementary criteria, imperative in terms of experimental feasibility and chemical consideration, had to be taken into account for the choice of such photolysis duration: (1) due to the weak electronic absorption of benzene at these wavelengths, the duration needed to be sufficiently long to observe spectral modification using a low-sensitivity in situ technique, that is, IR spectroscopy, and (2) to obtain only the formation of primary products.

We performed two different experiments: the first one reproduces fairly well the condensation sequence of ices in Titan's stratosphere, that is, benzene vapor was deposited onto the sample holder kept at 130 K. The temperature was maintained at 130 K for a few hours in order to insure a stable crystalline phase, and then cooled down to 70 K to prevent any desorption of benzene. The second experiment consisted of depositing benzene vapor at 70 K, followed by an annealing to 130 K before cooling to 70 K. These two experiments were performed in order to see if any differences are observed in the infrared spectrum due to the crystallization process. In addition, to identify the transition in the benzene ice phases from amorphous to crystalline, amorphous benzene was deposited at 16 K and then warmed-up to 300 K with several heating rates ranging between 0.5 and 2 K.min^{-1}. The ultimate goal of this experiment was to determine desorption temperature of solid benzene, with a quite accurate margin of variation supplied by the different heating rate, in our experimental conditions.

Sublimation is expected to happen at any temperature in a high vacuum chamber because, when an ice is formed, it is in equilibrium with the vapor phase. Since the chamber has turbo pumps, that vapor can continuously be pumped away, causing the ice to sublimate more and more over time. Nevertheless, this is a slow process at lower temperatures and this phenomenon is negligible at 70 K (see Figure 5), a temperature corresponding to the lowest one reached in the stratosphere of Titan. Furthermore, the choice of this temperature was all the more judicious. Indeed, in future experiments we will want to study co-condensed ices with different molecules, that is, HCN, which starts sublimating at around 80 K under our experi-

mental conditions. In both experiments, benzene is in the crystalline phase prior to the photolysis step, and the irradiation of benzene ice leads to the same photo-chemical activity of this molecule under our experimental conditions. Likewise, this temperature is sufficiently low to trap in the ice the photo-produced volatile fraction that will be characterized in a future work. Under these conditions of temperature (70 K), the subsequent benzene loss rate will only be attributed to photochemical processes, that is, avoiding any other competitive pathway such as sublimation. The evolution of the solid samples during irradiation was monitored by in situ infrared spectroscopy. After irradiation, ice samples are warmed up to 300 K with the cryogenic system switched-off in order to sublimate the photo-produced volatiles. The refractory organic residue is retained on the surface of the substrate.

3. Results

3.1. Benzene Ice

As the infrared data are poorly documented in the literature, it is necessary to study the thermal evolution of benzene in our experimental conditions to determine the evolution of the shape of its spectral features and its desorption/condensation temperature.

X-ray analysis supplemented by Fourier transform methods has shown the crystalline structure of benzene to be orthorhombic, with four molecules per unit (Bacon et al., 1964; Cox et al., 1958), the crystallographic parameters of which have also been determined. In this configuration, benzene molecules pack together like sheets of six-toothed gear wheels (Cox, 1958; Cox et al., 1958). The first member of the aromatic ring family, benzene belongs to the D_{6h} group and possesses 30 normal vibrational modes. Only two of them, namely A_{2u} (nondegenerate) and E_{1u} (degenerate), are infrared-active. However, the physical state of benzene can induce the activation of other vibrational modes (Halford & Schaeffer, 1946; Hollenberg & Dows, 1962), in particular for crystalline benzene, as explained by the development of intramolecular forces.

The solid benzene ice infrared spectrum was first studied by Halford and Schaeffer (1946) in the amorphous phase and then by numerous teams (Hollenberg & Dows, 1962; Mair & Hornig, 1949; Strazzulla & Baratta, 1991) in the crystalline phase. As we intend, in this study, to contribute to the interpretation of the VIMS-measured infrared spectra of aerosols present in Titan's stratosphere, we have chosen to focus on the six most intense absorption bands, the others being assigned to combination modes and/or harmonics, already detailed elsewhere (Bertie & Keefe, 2004; Mair & Hornig, 1949). The justification for this choice is that the quantities of benzene ice deposited in our experiments (and thus the resultant intensities of the IR signal) are much greater than those detected in Titan's atmosphere. Hence, it can be excepted that only the most intense benzene IR features would be detectable in Titan's IR spectra. Here, we present a study of the pure solid benzene infrared spectrum in both the amorphous and crystalline phases along with the vibrational assignments using Herzberg's notation (Herzberg, 1945).

3.1.1. Amorphous Pure Benzene Ice at 16 K

The infrared spectrum of amorphous benzene deposited at 16 K is shown in Figure 1. Wavenumbers of amorphous/crystalline benzene fundamental and combination modes observed in this study, along with their assignments (Bertie & Keefe, 2004; Herzberg, 1945; Mair & Hornig, 1949), are listed in Table 1. Intense absorption bands are observed below 1,500 cm^{-1}. First, the most intense one at 1,478 cm^{-1} corresponding to the $\nu C=C$ asymmetric stretching mode (ν_{13}), followed by the infrared features of two other fundamental vibrational modes at 1,035 cm^{-1} (ν_{14}) and at 674 cm^{-1} (ν_4), assigned to the δCH in-plane bending mode and the γCH out of plane bending mode, respectively. Another prominent absorption band characteristic of aromatic molecules, associated with the νCH stretching mode (ν_{12}), is located at 3,033 cm^{-1}. The most intense combination modes are attributed to $\nu_2+\nu_{13}+\nu_{18}$ and $\nu_{13}+\nu_{16}$ at 3,070 and 3,089 cm^{-1}, respectively.

3.1.2. Influence of Temperature on Pure Benzene Ices: Identification of Phase Transition and Desorption Processes

As the thermal evolution of solid benzene is rarely (Hollenberg & Dows, 1962; Ishii et al., 1996; Mair & Hornig, 1949) documented in the literature, we have studied the influence of temperature on the position and the shape of its infrared absorption bands. To monitor its phase transition by infrared spectroscopy, as previously described in the literature (Fraser et al., 2001; Koehler, 2001; Toumi et al., 2016), benzene ice was

Table 1
Positions and Assignments of the Most Intense Infrared Absorption Bands of Icy C_6H_6 at Different Temperatures

	Wavenumbers (cm^{-1})	
	This work	
Assignments (Herzberg, 1945)	T = 16 K amorphous ice	T = 70 K after 130 K crystalline ice
$\nu_{16} + \nu_{13}$, e_{1u}	3,089	3,092
		3,085
$\nu_2 + \nu_{18} + \nu_{16}$, e_{1u}	3,070	3,068
ν_{12}, e_{1u} CH aromatic stretching	3,033	3,038
		3,030
ν_{13}, e_{1u} C=C aromatic stretching	1,478	1,478
		1,475
ν_{12}, e_{1u} C–H in-plane bending	1,035	1,039
		1,033
ν_4, a_{2u} C–H out-of-plane bending	674	679

deposited at 16 K and then warmed up to 300 K with several heating rates (from 0.5 to 2 K.min^{-1}). Figure 2 presents the evolution of the surface coverage of C_6H_6 ν_{13} and ν_{14} modes with temperature and Figure 3 shows the infrared spectra of benzene as an amorphous ice and a crystalline one at various temperatures (cf. Table 1). These experiments were repeated three times and the variations observed on the surface coverage were less than 5% for a given temperature. The surface coverage Θ(T) of a vibrational mode corresponds to the value of the corresponding band peak area which has been normalized to the highest peak area value obtained from this band during the heat-up experiment. Benzene crystallization is observed around 55 K, which is consistent with works published earlier (Dawes et al., 2017; Ishii et al., 1996). Depending on the vibrational mode considered, during crystallization, the associated absorption band increases (ν_{14}, ν_4, $\nu_2 + \nu_{13} + \nu_{18}$) or decreases ($\nu_{13}$, ν_{12}, $\nu_{13} + \nu_{16}$) in intensity. No explanation of these trends has been found yet. Once the crystallization step has been initiated, C_6H_6 pure ice spectra show significant changes involving mainly the shift and the split of most infrared absorption bands, which become narrower. Above 3,000 cm^{-1}, the absorption band corresponding to ν_{12} is split into two bands as well as $\nu_{13} + \nu_{16}$ modes are split into two bands whereas the band for the $\nu_2 + \nu_{13} + \nu_{18}$ mode keeps the same profile, becoming thinner with respect to the amorphous ice. The band of the ν_{13} mode infrared signal is also split into two bands as well as the ν_{14} mode infrared feature. Shape modifications of this final vibrational mode as a function of temperature has already been demonstrated (Swenson et al., 1959). The ν_4 mode is shifted to higher frequencies but its shape looks almost identical. From 70 K to 130 K, no significant frequency shifts are observed and slight band intensity variations can be noted for all these modes. We observed that the surface coverage starts to decrease significantly around 145–150 K. Above 165 K, all the molecules desorb. We did not obtain any residue from pure C_6H_6 ice sublimation at room temperature.

3.2. Simulating Long-UV-Induced Aging of Benzene Ice Clouds in Titan's Stratosphere-Like Conditions

3.2.1. UV Absorption of Benzene and Dissociative Pathways

Several electronic absorption spectra of benzene in both liquid and gaseous phase have been published in the 200–300 nm range (Pantos et al., 1978; Suto et al., 1992). Recently, Dawes et al. (2017) published both amorphous and crystalline solid benzene (deposited under vacuum, 10^{-9} mbar) VUV spectra, compared with the gas phase VUV spectrum. Whatever the phase under consideration, the benzene electronic spectrum shows small absorption bands above 230 nm; however, when we performed irradiation at $\lambda > 230$ nm we irradiated through either singlet-singlet absorption ($^1B_{2u} \leftarrow {}^1A_{1g}$) or singlet-triplet absorptions ($^3E_{1u} \leftarrow {}^1A_{1g}$, $^3B_{2u} \leftarrow {}^1A_{1g}$) (Dawes et al., 2017).

Most laboratory experiments interested in the photochemical behavior of benzene have been carried out using lasers, leading to the formation of a solid polymer (Nakashima & Yoshihara, 1982) and C_6H_6 valence isomers (Griffith et al., 1975; Yokoyama et al., 1990). The latter have also been formed during the photolysis of benzene in cryogenic matrices at low temperature (Johnstone & Sodeau, 1991; Ruiterkamp et al., 2005; Toh et al., 2015). Fulvene, benzvalene, and Dewar benzene have been produced in argon or nitrogen matrix, when benzene was photolyzed at 253.7 nm or $\lambda > 230$ nm. Their theoretical infrared spectra have already been calculated with density functional theory calculations (Wheeless et al., 1995; Zhou & Liu, 1997).

The photolysis of adsorbed benzene at 105 K under KrF laser ($\lambda = 248$ nm) has demonstrated several dissociative pathways; absorption of one or two 248 nm photons induces the breaking of the CH bond causing the release of H° and $C_6H_5^{\bullet}$, only three-photon excitation triggers the aromatic ring opening, allowing the detection of C_2H_4 and C_2H_2 fragments by mass spectrometry (Varakin, 2018). In addition, Yoon et al. (2014)

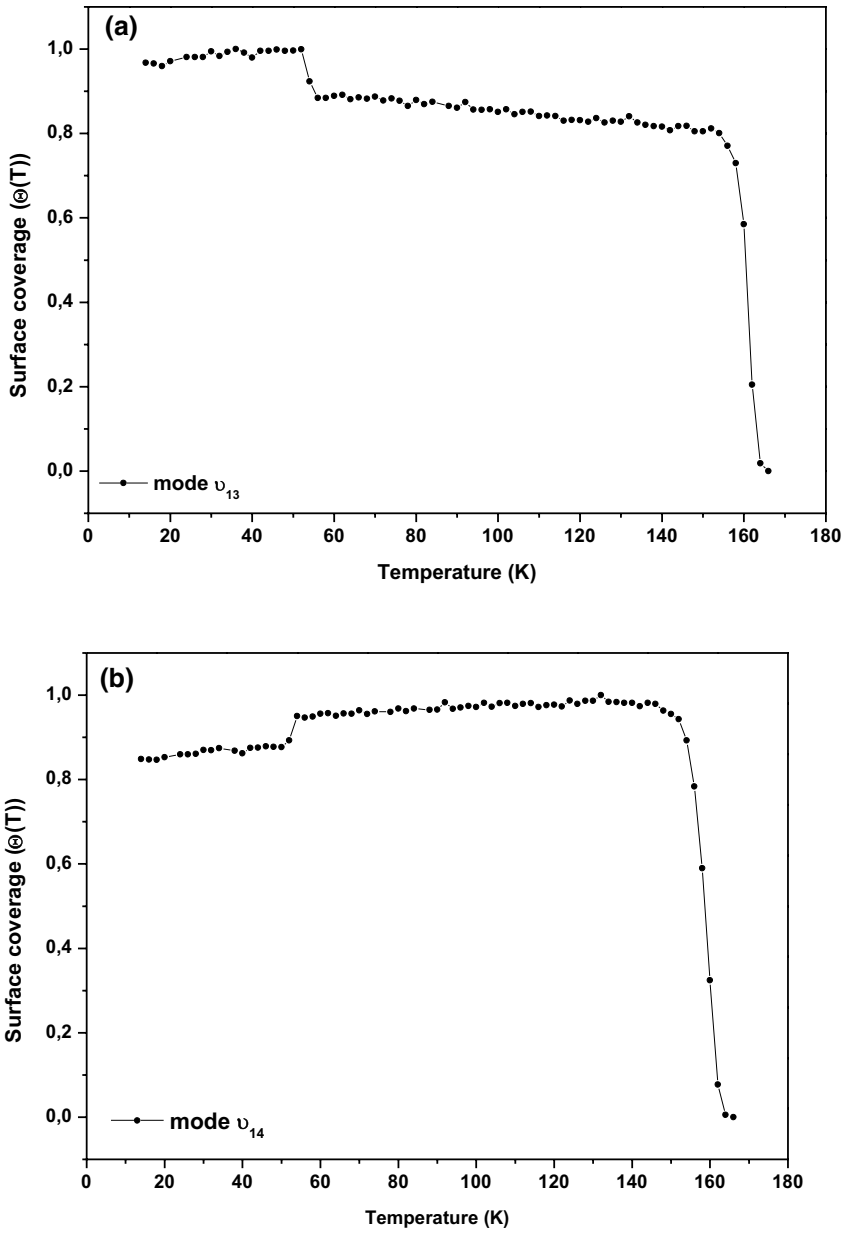

Figure 2. Surface coverage of C_6H_6 υ_{13} (a) and υ_{14} (b) modes as function of temperature (1.2 K.min^{-1}) determined by FTIR spectroscopy.

have suggested that $C_6H_5^{\bullet}$ and H° fragments, also produced at shorter wavelengths (λ = 193 nm), lead to the formation of aerosols.

3.2.2. Simulation of Benzene Photochemical Aging at Its Condensation Altitude

In order to understand the photochemical evolution undergone by stratospheric benzene condensates, pure benzene ices at 70 K were irradiated using a mercury lamp emitting at wavelengths $\lambda > 230$ nm, that is simulating solar photons that cross the stratosphere. As detailed in the experimental section, two types of deposition experiments were used to produce the benzene ice layer at 70 K. In a first experiment (case 1), the benzene ice was deposited at 70 K, then annealed to 130 K, then brought back down to 70 K. A second experiment (case 2) consisted in depositing the ice at 130 K and then cooling it down to 70 K. During the pho-

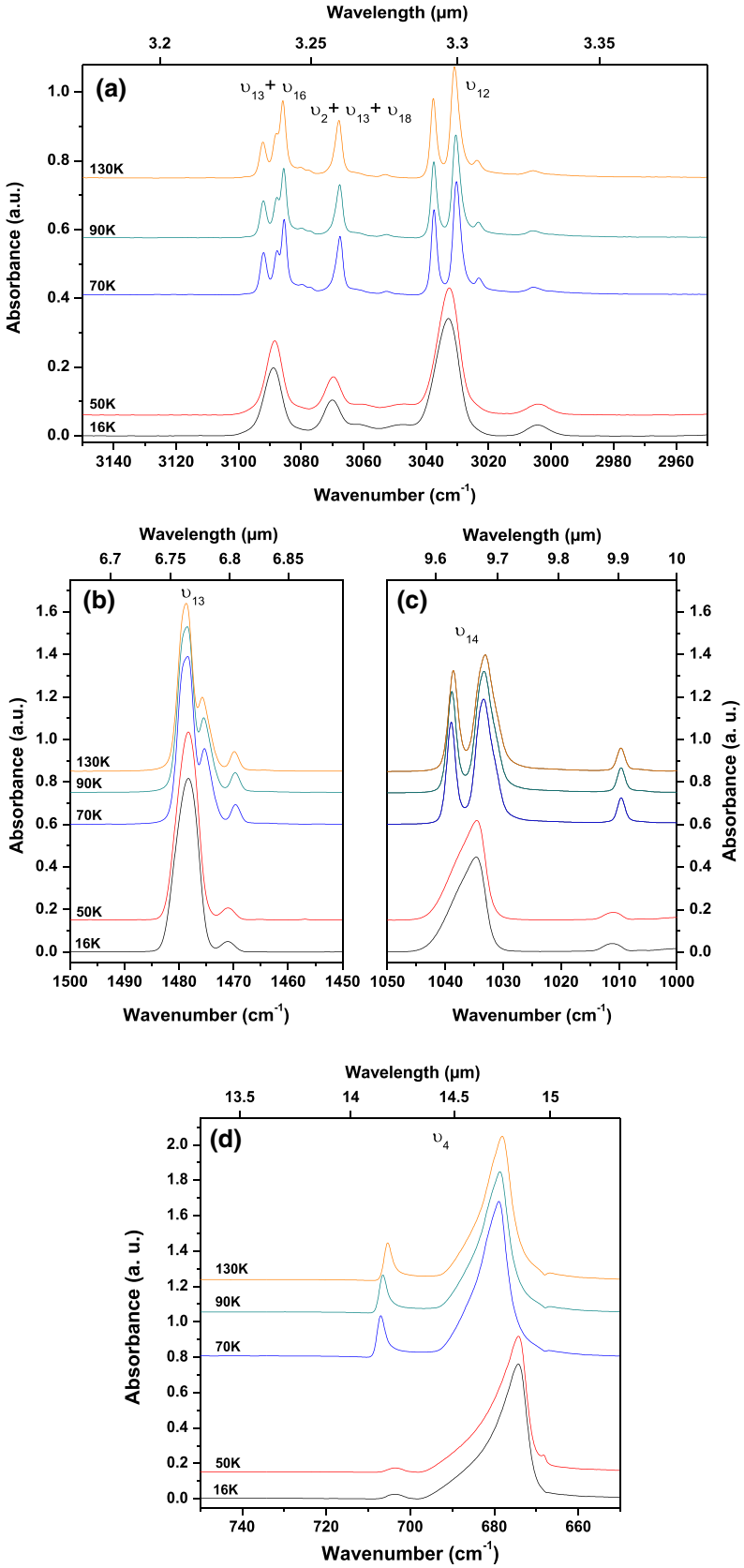

Figure 3. Infrared spectra of C_6H_6 (amorphous ice) (16 K and 50 K) and (crystalline ice) (70 K, 90 K, and 130 K) in different areas labeled (a–d) characteristics of the most intense bands of the benzene ice.

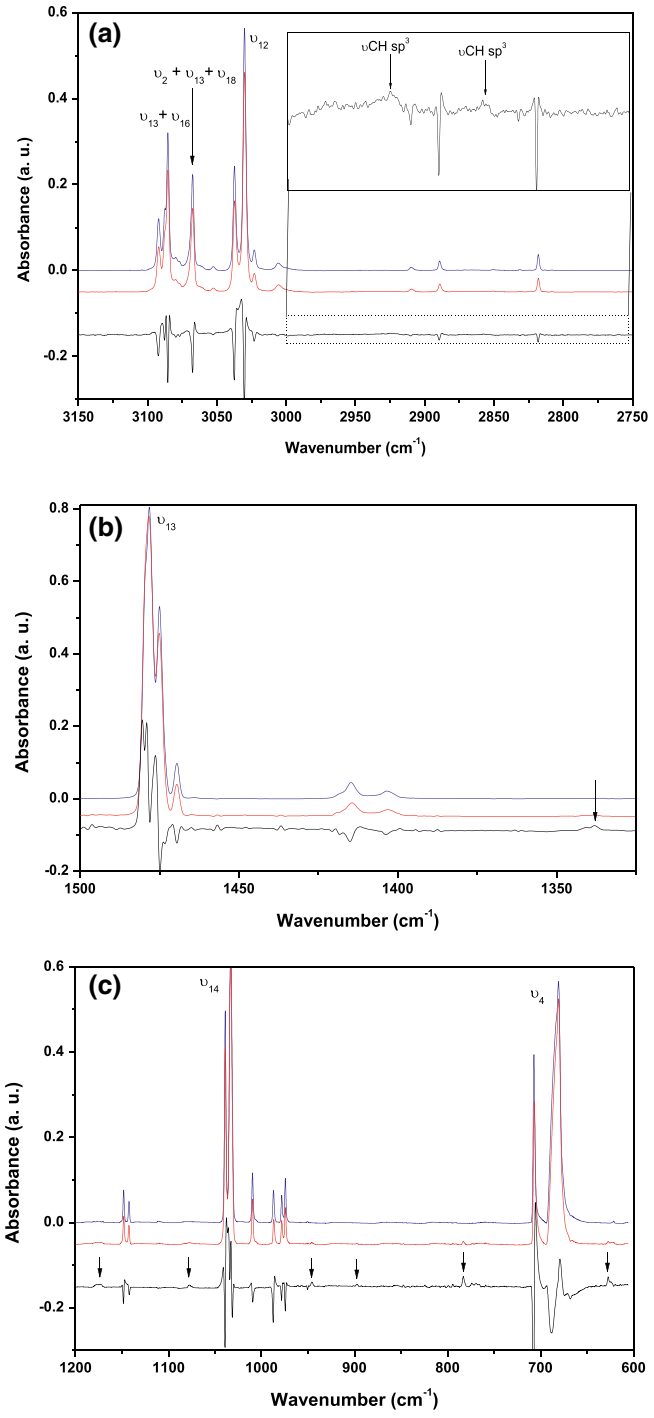

Figure 4. FTIR spectra of C_6H_6 at 70 K (case 1), presented in different areas (a) between 3,150 and 2,750 cm^{-1}, (b) between 1,500 and 1,300 cm^{-1}, (c) between 1,200 and 600 cm^{-1}): (blue)/(red) before/after 2,880 min of irradiation ($\lambda > 230$ nm) and (black) subtraction spectrum multiplied by a factor of 3. Arrows highlight the new photo-produced spectral features corresponding to the fulvene isomer. For the interpretation of the legend, the reader must refer to the web version of this article.

tolysis of these two resulting ices, benzene absorption bands decreased in intensity, as displayed in Figure 4 (this experiment corresponds to case 1). The evolution of most benzene vibrational modes as a function of time cannot be fitted by any-order kinetic rate, because of new spectral features growing at their edge. However, the combination mode $\nu_2+\nu_{13}+\nu_{18}$ peaking at 3,068 cm^{-1} provides an exception to these observations, and its evolution over time can be fitted by a first-order kinetic rate, as shown in Figure 5, giving a kinetic constant of $(6.4 \pm 0.5).10^{-4}$ min^{-1} (case 1) or $(7.7 \pm 1.3).10^{-4}$ min^{-1} (case 2). Hence, no significant variation on the kinetic constant value is observed from the results of both cases. As the photon flux of our lamp is about 2.34×10^{16} photon.cm^{-2}.s^{-1}, the corresponding photo-dissociation cross-section is estimated to be 4.6×10^{-22} photons.cm^{-2} (case 1) and 5.5×10^{-22} photons.cm^{-2} (case 2). This value of the benzene photo-dissociation cross-section is probably a consequence of radical recombinations and slow diffusion processes, etc. Indeed, at low temperature, the mobility of molecules and heavy radicals is low while H° radicals can locally diffuse through the benzene ice's bulk.

After 2,880 min of irradiation, 14±5% of the C_6H_6 is consumed. The infrared features that grow at the edge of the benzene absorption bands (observed in cases 1 and 2) can be assigned to two different mechanisms: amorphization or polymerization. Figure 6 compares the subtraction infrared spectrum at 70 K of the benzene ice (case 1) after-before UV photolysis with the infrared spectrum of amorphous benzene ice (50 K). The peaks marked with asterisks, on the left side of the figure, correspond to amorphous benzene features while the ones, marked with triangles, on the right side, are characteristic of the formation of polymeric material, as has already been highlighted by Couturier-Tamburelli et al. (2015, 2018), in the case of HC_5N or HC_3N photolysis.

In addition to these two pathways, we observed the formation of new absorption bands, whose frequencies are listed in Table 2. The weak bands at 2,930 and 2,855 cm^{-1} indicate the formation of aliphatic compounds, corresponding, respectively, to a CH_2 asymmetric and symmetric stretching mode (Carpentier et al., 2012; Imanaka et al., 2004; Sciamma-O'Brien et al., 2017). Several absorption bands below 1,400 cm^{-1} are found at 1,341, 1,338, 1,078, 946, 898, 783, and 627 cm^{-1} (case 1). Except the band at 898 cm^{-1}, these others bands are also observed during the photolysis of the benzene ice obtained from the case 2 (cf. Figure 7). Because the 898 cm^{-1} peak is the least intense in that spectral region, it is possible that, for the case 2 experiment, its intensity was below the detection threshold of the IR spectrometer. In the literature, the photo-excitation of benzene is known to result in the formation of valence isomers. These photoproducts have been identified in particular during the photolysis of benzene isolated in cryogenic matrices. However, the IR spectra of the same species in an amorphous or crystalline phase are unknown to our knowledge. Referring to the study of Johnstone and Sodeau (1991), the IR features of fulvene (5-methylenecyclopenta^{-1},3-diene), one of benzene's valence isomers, could correspond to the ones obtained from the photolysis of the benzene ice. Indeed, in this study the benzene was isolated in an argon matrix and irradiated with UV $\lambda > 230$ nm, so we can consider frequency shifts due to differences in the chemical environment between the matrix and the ice experiments. In order to confirm this hypothesis, benzene isolated in a nitrogen matrix was irradiated ($\lambda > 230$ nm), then softly warmed up (Figure S1). This last step induces the sublimation of

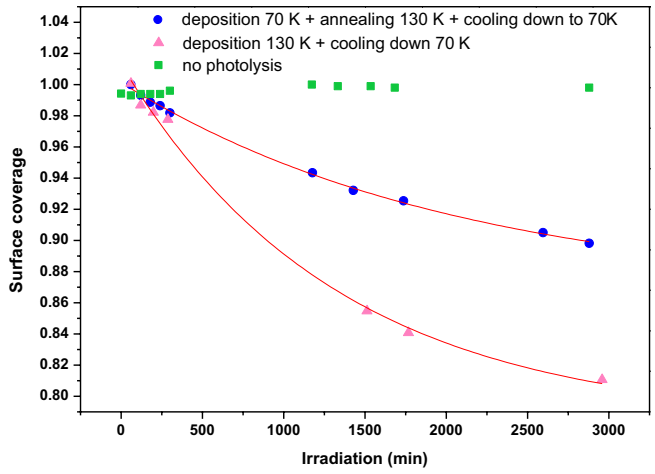

Figure 5. Evolution of the surface coverage of the benzene $\nu_2 + \nu_{13} + \nu_{18}$ combination mode at 70 K for nonirradiated ice (squares), and during irradiation for ice deposited at 70 K, annealed to 130 K and cooling down to 70 K (circles, case 1) and ice deposited at 130 K and cooled to 70 K (triangles, case 2). The decrease is fitted by a single exponential decay.

the matrix gas (N_2) around 35 K, resulting in the obtention of an amorphous benzene ice in which the photo-products formed in the matrix, and more precisely the fulvene, were trapped. A subsequent warm up to 70 K allowed for the experimental IR spectra of solid fulvene, to be measured. We have compared this spectrum with our experimental solid state data. The experimental frequencies are compared, in Table 2, to those of solid state and in situ matrix-produced fulvene (Figure S1). The comparison of these new absorption band frequencies with those obtained after nitrogen matrix sublimation confirms the formation of fulvene in irradiated C_6H_6 ices.

3.2.3. Infrared Characterization of Benzene Ice Residues

At the end of the photolysis experiment, we performed a warming-up to allow nonirradiated benzene monomers as well as volatile photoproducts, such as fulvene, to be released as gases. This step allows the in situ characterization of the refractory polymer produced by photochemistry. Under our experimental conditions, a small amount of nonvolatile residue was observed after the warm up. The residue obtained corresponds to an organic material which has a brownish color, reminiscent of Titan's haze, and is soluble in dichloromethane, as observed for laboratory analogs of high-altitude aerosols soluble in methanol, another polar solvent (Carrasco et al., 2009).

The infrared spectrum of the benzene residue is presented in Figure 8 and shows the presence of a broad and well-structured band in the 3,350–2,750 cm^{-1} region, along with a band at 1,404 cm^{-1} that could be assigned to semi-circle stretching of aromatics rings (Larkin, 2011). Higher intensities are observed for the peaks located above 3,000 cm^{-1}, corresponding to νCH sp^2 stretching modes, in comparison to the peaks below 3,000 cm^{-1}, assigned to νCH sp^3 stretching modes. As this cluster is the result of the overlap of several absorption bands, a deconvolution into Gaussian components was performed in order to characterize

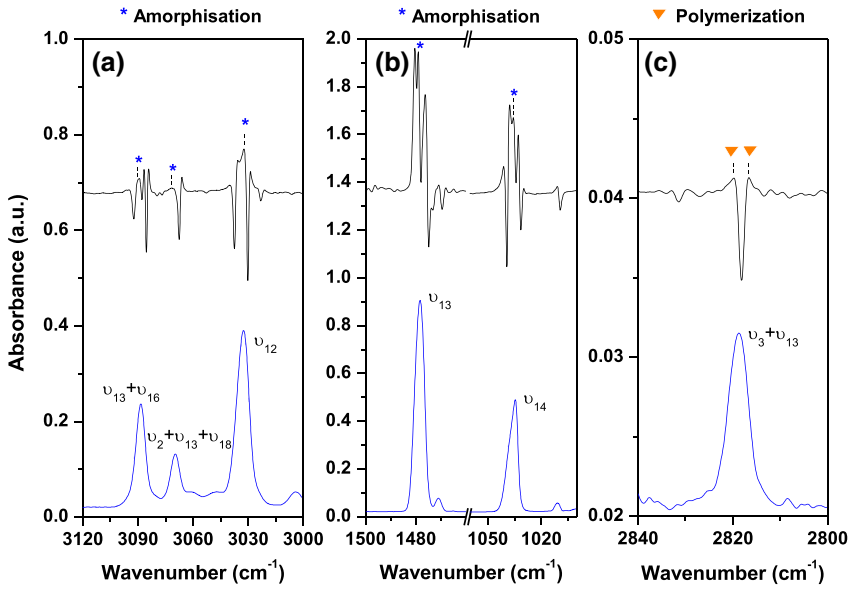

Figure 6. Comparison of the subtraction FTIR spectrum (after-before UV irradiation) of case 1 benzene ice at 70 K (top), with the infrared spectrum of amorphous benzene ice at 50 K (bottom), in different spectral regions (a) between 3,120 and 3,000 cm^{-1}, (b) between 1,500 and 1,000 cm^{-1}, (c) between 2,840 and 2,800 cm^{-1}). Peaks marked with asterisks correspond to amorphous benzene features while features characteristic of polymerization are marked with triangles.

Table 2
Positions and Assignments of New Infrared Absorption Bands Obtained During the Photolysis of C6H6 Ice (λ > 230 nm) at 70 K, Compared with the Infrared Features of Fulvene in the Solid State and in Cryogenic Matrices

				Solid fulvene bands (cm^{-1})		Matrix-isolated fulvene bands (cm^{-1})	
Wavenumbers (cm^{-1})	Wavelengths (μm)	Assignments	Tentative assignment	After irradiation of benzene ice (this work)	After sublimation of nitrogen matrix	N_2	Ar[e]
2,930	3.41	Asymmetric stretching CH_2[a,b]	Residue aliphatic groups	-	-	-	-
2,855	3.5	Symmetric stretching CH_2[c]	Residue aliphatic groups	-	-	-	-
1,341	7.46	In-plane bending CH[d]	Fulvene	1,339	1,339	1,343.6	1,342.8
1,338	7.47						
1,078	9.28	In-plane bending CH/C-C-C in-plane bending[d]	Fulvene	1,076	1,076	1,080.7	
946	10.6	Ring in-plane deformation + C-C stretching[d]/out-of-plane bending CH[d]	Fulvene	939	939	932.4	926.3
898	11.1	Ring in-plane deformation/C-C stretching[d]	Fulvene	896	896	894.0	894.5
783	12.8	Out-of-plane bending CH[d]	Fulvene	778	778	773.0	770.6
627	15.9	Out-of-plane bending aromatic CH_2[d]	Fulvene	622	622	617.8	616.3

[a]Imanaka et al. (2004). [b]Sciamma-O'Brien et al. (2017). [c]Carpentier et al. (2012). [d]Wheeless et al. (1995). [e]Johnstone & Sodeau, (1991).

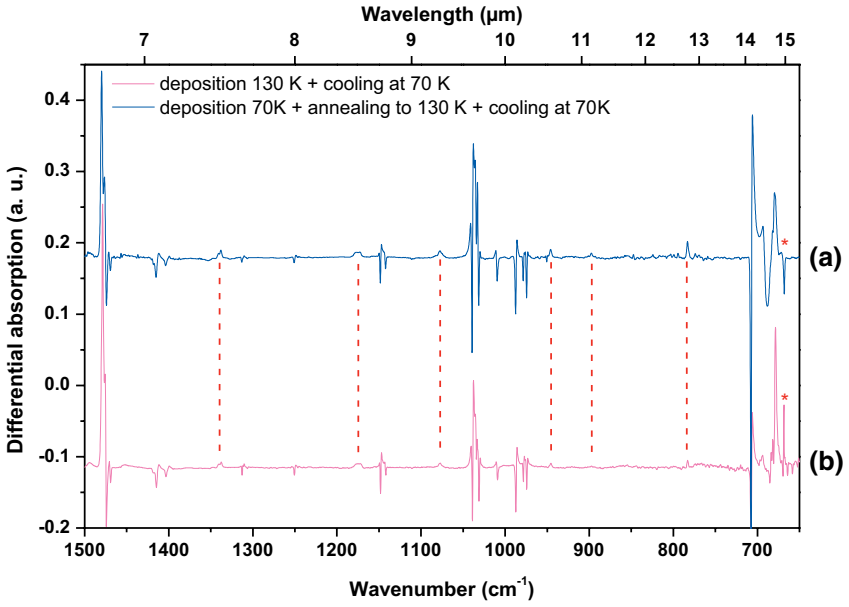

Figure 7. Comparison of the subtraction spectrum (after-before UV irradiation experiments) for both cases 1 and 2 benzene ice deposition conditions: (a) deposition 70 K followed by an annealing to 130 K and then cooling at 70 K (case 1) (b) deposition at 130 K followed by a cooling down to 70 K (case 2); *CO_2 (g): dashed lines photo-produced absorption bands common to both experiments.

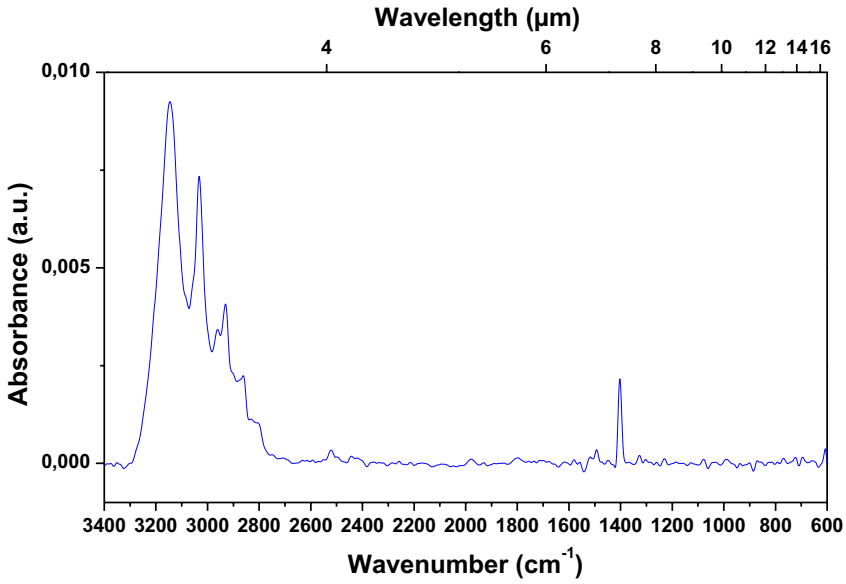

Figure 8. FTIR spectra recorded at 300 K of the residue produced by UV radiations ($\lambda > 230$ nm) of C_6H_6 ice at 70 K followed by a warm-up to 300 K.

each of them, as presented in Figure 9. Their respective assignments are reported in Table 3. During the fitting process, we set positions as free parameters, as in previous studies (Carrasco et al., 2018). Taking into account previous works concerning both the influence of benzene in the chemical composition of tholins (Sciamma-O'Brien et al., 2017) and the spectroscopic characterization of hydrogenated amorphous carbon-based structures (Dartois et al., 2004), only two vibrational modes are exclusive to this study, the others being common to the studies cited above.

The Gaussian component at 3,213 cm^{-1} could be assigned to CH stretching modes from conjugated alkyne derivatives which could explain the frequency shift toward lower energies with respect to the one observed in alkyne functions (Larkin, 2011). The intense 3,144 cm^{-1} peak could result from a CH sp^2 stretching mode from a derivative/substituted polyphenyl compound (Ghanem et al., 1987). Aromatic and vinylic -CH_2 asymmetric stretching modes are centered at 3,086 cm^{-1} (Sciamma-O'Brien et al., 2017) while CH stretching modes from the aromatic/alkene family are found at 3,060, 3,031, and 2,999 cm^{-1} (Sciamma-O'Brien et al., 2017). By means of previous studies (Imanaka et al., 2004; Quirico et al., 2008; Sciamma-O'Brien et al., 2017), -CH_3 asymmetric and symmetric stretching modes are assigned to the Gaussian component at 2,964 and 2,863 cm^{-1} respectively against 2,930 and 2,829 cm^{-1} for -CH_2 group (Larkin, 2011). A last peak has been found at 2,894 cm^{-1} which could be assigned either to the sp^3 νCH stretching mode or to the -CH_2 Fermi resonance (Carpentier et al., 2012) or the asymmetric -CH_2 wing mode (Dartois et al., 2004). This last vibrational mode presents its symmetric counterpart at 2,800 cm^{-1} (Dartois et al., 2004).

4. Discussion

Vapor condensation of benzene in Titan's stratosphere, modeled in different works, leads to the formation of icy particles whose formation altitude depends on climatic conditions as well as abundances. Based on different models, the condensation of benzene is expected at 85 km for a temperature of about 130 K (Barth, 2017; Lavvas et al., 2011). At these altitudes, ices can evolve according to two main pathways; the first one consists of the adsorption of condensable species and the second one is triggered by photochemical reactions induced by long-UV solar photons. For benzene, which is a key molecule at high altitude in the formation of both the complex organics and aerosols that cover Titan's surface, none of these processes have been experimentally investigated in stratospheric-like conditions. Hence, the role played by benzene ices in this part of the atmosphere has not been clearly identified so far. In this study, we have shown the photo-

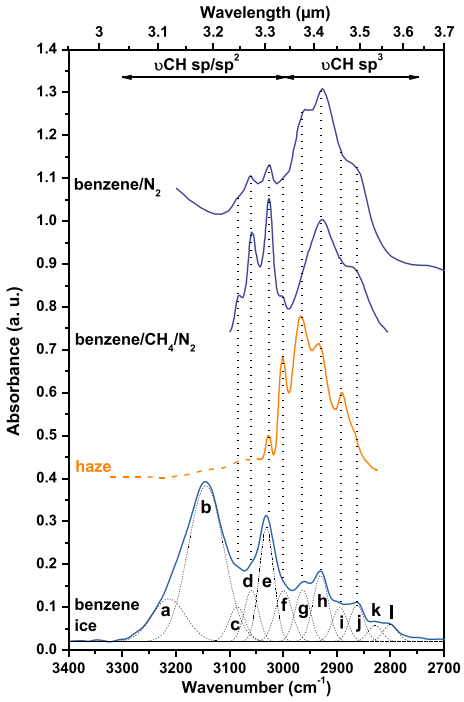

Figure 9. Deconvolved infrared spectrum of irradiated benzene ice residue (bottom, blue line) produced by photochemistry ($\lambda > 230$ nm) and subsequently warmed up to room temperature compared with VIMS solar occultation spectrum at 203 km altitude (Bellucci et al., 2009; Kim et al., 2011) (orange solid line, processed by Carrasco et al. [2018] from Kim et al. [2011] between 3,050 and 2,825 cm^{-1}, and orange dashed line corresponds to Titan's haze spectra from Kim et al. [2011] above 3,050 cm^{-1}). The experimental spectrum is also compared with the IR spectra of aerosols generated from a N_2:C_6H_6 gas mixture submitted to UV irradiation (Gautier et al., 2017) (top, blue) or from a N_2:CH_4:C_6H_6 gas mixture in a cold plasma discharge (Sciamma-O'Brien et al., 2017). For the interpretation of the legend, the reader must refer to the web version of this article.

chemical activity of benzene ice under long-UV irradiation ($\lambda > 230$ nm) which results in the formation of volatile photoproducts, in particular fulvene—detected by IR spectroscopy—and a refractory material, that can be considered as an analogue of aerosols formed in Titan's atmosphere. At 70 K, it takes 48 h to lose almost 14±5 % of the benzene in our experiment. However, as the solar flux reaching Titan's stratosphere is around 10^{14} photon.cm^{-2}.s^{-1}, the same depletion rate for benzene will be achieved after 2.6 Earth years on Titan. Even though we present the photochemistry of benzene at a lower temperature (70 K) than the one at which it is expected to condense, our results demonstrate a low dissociation rate of benzene under stratospheric conditions. Hence, most of the benzene ice would not be modified by the solar UV photons that penetrate the stratosphere. With small increases in temperature induced, for example, by transportation to higher altitudes, all photo-produced volatiles species and benzene undergo thermal desorption observed between 160 and 190 K depending on whether the experiments were carried out under vacuum or at 10^{-2} mbar leaving only the residue in the solid state, depending on the season in Titan's atmosphere. So, we can assume that in this condition the photoproducts formed in solid phase could be released in the stratosphere during climatic condition variations.

The formation of aerosols produced by the photochemistry of gas phase benzene under more energetic conditions, relevant for simulating the chemistry occurring at higher altitudes in Titan's atmosphere, has been experimentally investigated in other groups (Gautier et al., 2017; Sciamma-O'Brien et al., 2017; Trainer et al., 2013). In Figure 9, our experimental spectrum of the benzene residue is compared with the IR spectra of aerosols generated with a N_2:C_6H_6 gas mixture submitted to UV irradiation (Gautier et al., 2017 top, blue) or by a N_2:CH_4:C_6H_6 gas mixture in a cold plasma discharge (Sciamma-O'Brien et al., 2017). Figure 8 also shows a comparison of our experimental spectrum to observational data of Titan's atmosphere at ~200 km supplied by the VIMS spectrometer (lowest altitude, where a well-resolved spectrum is observed) (Bellucci et al., 2009; Carrasco et al., 2018; Kim et al., 2011). In their study, Kim et al. retrieved the detailed spectral feature using a radiative transfer program including absorption and scattering by haze particles. The spectral features of the haze retrieved from the VIMS data at various altitudes are similar to each other, indicating relatively uniform spectral properties of the haze with altitude. The observations were carried out on January 15, 2006 during the solar egress at 71°S (Bellucci et al., 2009).

As observed in Figure 9, it is in the spectral region characteristic of aromatic structures that we have found major discrepancies. Indeed, the most intense band observed at 3,144 cm^{-1} in our residue matches only with the very small VIMS-observed spectral signature of stratospheric aerosols, in terms of position but not in intensity. On the other hand, our deconvolved bands at 3,086, 3,060, 3,031, and 2,999 cm^{-1} are common to those observed in these other laboratory-produced aerosols and the VIMS data. Their relative intensities correspond rather well to the bands observed in the other aerosols. In particular, the greatest intensities observed for these bands mimic the ones observed in the aerosols produced from the N_2:CH_4:C_6H_6 gas mixture (Sciamma-O'Brien et al., 2017)

In addition, from 3,000 to 2,850 cm^{-1}, we found a similar spectral profile, indicating that similar aliphatic structures obtained in all the laboratory experiments are in good agreement with those of Titan's haze. That said, it is important to keep in mind that none of these selected experimental works leads to aerosol analogs which present IR features that are strictly identical to Titan's aerosols ones. However, the relative intensity of these aliphatic structures to the aromatics in our residue are low compared with other experimental data and the observation. Nevertheless, these relative proportions are close to those produced in the cold plasma

Table 3
Deconvolved Infrared Absorption Bands of C6H6 Residue in the 3,150–2,750 cm^{-1} Region

Label	Wavenumbers (cm^{-1})	Wavelengths (μm)	Assignments
a	3,213	3.12	sp -CH stretching (conjugated alkyne ?)[d]
b	3,144	3.18	sp^2 -CH stretching (derivative/substituted polyphenyl ?)[e]
c	3,086	3.24	sp^2 asymmetric -CH_2 stretching (aromatic/alkene) [b, c]
d	3,060	3.26	sp^2 -CH stretching (aromatic) [b]
e	3,031	3.30	sp^2 -CH stretching (aromatic) [b]
f	2,999	3.33	sp^2 -CH stretching (aromatic/alkene) [b]
g	2,964	3.37	sp^3 asymmetric CH_3 stretching (alkane/aliphatic) [a, b]
h	2,930	3.41	sp^3 asymmetric CH_2 stretching (alkane/aliphatic) [a, b]
i	2,894	3.46	sp^3 -CH stretching [f]/-CH_2 Fermi resonance [f]/sp^2 asymmetric CH_2 wing [c]
j	2,863	3.49	sp^3 symmetric CH_3 stretching (alkane/aliphatic) [b]
k	2,829	3.53	sp^3 symmetric CH_2 stretching (alkane/aliphatic) [d]
l	2,800	3.57	sp^2 symmetric CH_2 wing[c]

[a]Imanaka et al. (2004). [b]Sciamma-O'Brien et al. (2017). [c]Dartois et al. (2004). [d]Larkin, (2011). [e]Ghanem et al. (1987). [f]Carpentier et al. (2012).

discharge. As a consequence, the polymeric structure that has been produced by the exposure of a benzene ice to long-UV irradiation (70 K) may present similar aromatic/aliphatic groups—in terms of structures and proportions—to the aerosols generated by plasma discharge (initiated at 150 K) that simulate higher altitudes in the atmosphere. As these aerosols analogs from our study and from the Sciamma-O'Brien et al. (2017) and Gautier et al. (2017) studies have not been produced with the same temperature conditions, the analogs formation could be temperature dependent.

However, several deconvolved absorption bands of the benzene residue, namely at 3,213, 2,829 and 2,800 cm^{-1}, are not observed among the infrared features of Titan's haze observed in the stratosphere. In our study, the benzene residue formed in our experiments results from photo-processed ices without considering further aging processes such as that induced by the accretion of condensates at their surface. In addition, Courtin et al. (2015) demonstrated the coating of condensates below 300 km could impact the ratio between aromatics and aliphatics. In addition, experimental works performed by Couturier-Tamburelli et al. (2018) highlighted a possibility of photo-insertion of hydrogen atoms into a nitrile-based residue coated with HCN ice. Therefore, it will be of interest to investigate the coating effects on the spectral features assigned to –CH stretching modes of benzene residues. However, if the 3,144 cm^{-1} absorption band, characteristic of benzene photochemistry, is normalized to the intensity of the corresponding band from VIMS observations, we can assume that the contribution of benzene aerosols was very low in Titan's atmosphere at the time the measurement was performed. It demonstrates that other kinds of aerosols, present in the stratosphere, explain the high intensity of aliphatic CH contributions. In fact, in our experiment, the residue is produced by photo-processed hydrogen-bearing carbonaceous ices, while in Titan's stratosphere the haze probed by Cassini VIMS spectrometer results from the complex photochemistry of hydrocarbons and nitriles. Nevertheless, these preliminary laboratory experiments constitute a first step in understanding the role played by benzene ices in the formation of gaseous species and aerosols in the stratosphere that will subsequently be transported to the surface. It will thus allow the experimental simulation of a more complex benzene-containing cloud to better understand their photochemical evolution at these altitudes as well as their contribution to the surface organic layer.

5. Conclusion

To understand the fate of benzene ices in Titan's stratosphere, we turned to laboratory experiments to simulate its photochemical evolution triggered by long-UV irradiation ($\lambda > 230$ nm). Our results demonstrate a photochemical activity of benzene which leads to the formation of volatile photo-products, in particular

fulvene, as well as a solid residue, that is, a laboratory analog of benzene aerosols. Its spectroscopic characterization highlights a good correlation with VIMS observations for the positions of most of the deconvolved absorption bands, in particular for the features that correspond to aliphatic groups, which does not hold for the relative intensities of CH sp^2/sp^3 ratio obtained in the residue when warming up the irradiated ice to 300 K. Therefore, the photochemistry of benzene ice might lead to the formation of organic materials that will contribute to the composition of the haze and to the organic material present on Titan's surface which will be investigated by the future Dragonfly space mission. Moreover, this study will also help to establish points of comparison with the changes that may be observed when benzene is co-condensed with another molecule like HCN.

Data Availability Statement

The data used from in this article are available on zenodo data repository http://doi.org/10.5281/zenodo.4350657s

Acknowledgments
This work was funded by the French national program "PNP." The authors thank Dr. Grégoire Danger for the technical support on the AHIIA experiment. The authors would like to express their sincere gratitude to J. Noble for help in correcting the manuscript and referees to improve it.

References

Abplanalp, M. J., Frigge, R., & Kaiser, R. I. (2019). Low-temperature synthesis of polycyclic aromatic hydrocarbons in Titan's surface ices and on airless bodies. *Science Advances*, *5*(10), eaaw5841. https://doi.org/10.1126/sciadv.aaw5841

Anderson, C. M., Samuelson, R. E., & Nna-Mvondo, D. (2018). Organic ices in Titan's stratosphere. *Space Science Reviews*, *214*(8), 125. https://doi.org/10.1007/s11214-018-0559-5

Anderson, C. M., Samuelson, R. E., Yung, Y. L., & McLain, J. L. (2016). Solid-state photochemistry as a formation mechanism for Titan's stratospheric C4N2 ice clouds. *Geophysical Research Letters*, *43*(7), 3088–3094. https://doi.org/10.1002/2016GL067795

Bacon, G. E., Curry, N. A., Wilson, S. A., & Spence, R. (1964). A crystallographic study of solid benzene by neutron diffraction. *Proceedings of the Royal Society of London. Series A. Mathematical and Physical Sciences*, *279*(1376), 98–110. https://doi.org/10.1098/rspa.1964.0092

Bampasidis, G., Coustenis, A., Achterberg, R. K., Vinatier, S., Lavvas, P., Nixon, C. A., et al. (2012). Thermal and chemical structure variations in Titan's stratosphere during Cassini Mission. *The Astrophysical Journal*, *760*(2), 144. https://doi.org/10.1088/0004-637X/760/2/144

Barth, E. L. (2017). Modeling survey of ices in Titan's stratosphere. *Planetary and Space Science*, *137*, 20–31. https://doi.org/10.1016/j.pss.2017.01.003

Barth, E. L., & Toon, O. B. (2003). Microphysical modeling of ethane ice clouds in Titan's atmosphere. *Icarus*, *162*(1), 94–113.

Bellucci, A., Sicardy, B., Drossart, P., Rannou, P., Nicholson, P., Hedman, M., et al. (2009). Titan solar occultation observed by Cassini/VIMS: Gas absorption and constraints on aerosol composition. *Icarus*, *201*(1), 198–216.

Bertie, J. E., & Keefe, C. D. (2004). Infrared intensities of liquids XXIV: optical constants of liquid benzene-h6 at 25 °C extended to 11.5 cm^{-1} and molar polarizabilities and integrated intensities of benzene-h6 between 6200 and 11.5 cm^{-1}. *Journal of Molecular Structure*, *695–696*, 39–57. https://doi.org/10.1016/j.molstruc.2003.11.002

Butscher, T., Duvernay, F., Theule, P., Danger, G., Carissan, Y., Hagebaum-Reignier, D., & Chiavassa, T. (2015). Formation mechanism of glycolaldehyde and ethylene glycol in astrophysical ices from HCO˙ and ˙CH_2 OH recombination: an experimental study. *Monthly Notices of the Royal Astronomical Society*, *453*(2), 1587–1596. https://doi.org/10.1093/mnras/stv1706

Callahan, M. P., Gerakines, P. A., Martin, M. G., Peeters, Z., & Hudson, R. L. (2013). Irradiated benzene ice provides clues to meteoritic organic chemistry. *Icarus*, *226*(2), 1201–1209. https://doi.org/10.1016/j.icarus.2013.07.033

Carpentier, Y., Féraud, G., Dartois, E., Brunetto, R., Charon, E., Cao, A.-T., et al. (2012). Nanostructuration of carbonaceous dust as seen through the positions of the 6.2 and 7.7 μ m AIBs. *Astronomy & Astrophysics*, *548*, A40. https://doi.org/10.1051/0004-6361/201118700

Carrasco, N., Schmitz-Afonso, I., Bonnet, J.-Y., Quirico, E., Thissen, R., Dutuit, O., et al. (2009). Chemical characterization of Titan's tholins: Solubility, morphology and molecular structure revisited. *The Journal of Physical Chemistry A*, *113*(42), 11195–11203.

Carrasco, N., Tigrine, S., Gavilan, L., Nahon, L., & Gudipati, M. S. (2018). The evolution of Titan's high-altitude aerosols under ultraviolet irradiation. *Nature Astronomy*, *2*, 489–494. https://doi.org/10.1038/s41550-018-0439-7

Cordiner, M. A., Palmer, M. Y., Nixon, C. A., Irwin, P. G. J., Teanby, N. A., Charnley, S. B., et al. (2015). Ethyl cyanide on Titan: Spectroscopic detection and mapping using Alma. *The Astrophysical Journal Letters*, *800*(1), L14.

Courtin, R., Kim, S. J., & Bar-Nun, A. (2015). Three-micron extinction of the Titan haze in the 250–700 km altitude range: Possible evidence of a particle-aging process. *Astronomy & Astrophysics*, *573*, A21. https://doi.org/10.1051/0004-6361/201424977

Coustenis, A., Achterberg, R. K., Conrath, B. J., Jennings, D. E., Marten, A., Gautier, D., et al. (2007). The composition of Titan's stratosphere from Cassini/CIRS mid-infrared spectra. *Icarus*, *189*(1), 35–62. https://doi.org/10.1016/j.icarus.2006.12.022

Coustenis, A., Jennings, D. E., Achterberg, R. K., Bampasidis, G., Lavvas, P., Nixon, C. A., et al. (2016). Titan's temporal evolution in stratospheric trace gases near the poles. *Icarus*, *270*, 409–420. https://doi.org/10.1016/j.icarus.2015.08.027

Coustenis, A., Jennings, D. E., Achterberg, R. K., Bampasidis, G., Nixon, C. A., Lavvas, P., et al. (2018). Seasonal evolution of Titan's stratosphere near the poles. *The Astrophysical Journal*, *854*(2), L30. https://doi.org/10.3847/2041-8213/aaadbd

Coustenis, A., Jennings, D. E., Nixon, C. A., Achterberg, R. K., Lavvas, P., Vinatier, S., et al. (2010). Titan trace gaseous composition from CIRS at the end of the Cassini–Huygens prime mission. *Icarus*, *207*(1), 461–476. https://doi.org/10.1016/j.icarus.2009.11.027

Coustenis, A., Salama, A., Schulz, B., Ott, S., Lellouch, E., Encrenaz, T. h, et al. (2003). Titan's atmosphere from ISO mid-infrared spectroscopy. *Icarus*, *161*(2), 383–403. https://doi.org/10.1016/S0019-1035(02)00028-3

Couturier-Tamburelli, I., Piétri, N., & Gudipati, M. S. (2015). Simulation of Titan's atmospheric photochemistry: Formation of non-volatile residue from polar nitrile ices. *Astronomy & Astrophysics*, *578*, A111. https://doi.org/10.1051/0004-6361/201425518

Couturier-Tamburelli, I., Piétri, N., Letty, V. L., Chiavassa, T., & Gudipati, M. (2018). UV–vis light-induced aging of Titan's haze and ice. *The Astrophysical Journal*, *852*(2), 117. https://doi.org/10.3847/1538-4357/aa9e8d

Cox, E. G. (1958). Crystal structure of benzene. *Reviews of Modern Physics*, *30*(1), 159–162. https://doi.org/10.1103/RevModPhys.30.159

Cox, E. G., Cruickshank, D. W. J., & Smith, J. A. S. (1958). The crystal structure of benzene at -3 C. *Proceedings of the Royal Society of London. Series A, Mathematical and Physical Sciences*, *247*(1248), 1–21.
Cui, J., Yelle, R. V., Vuitton, V., Waite, J. H., Kasprzak, W. T., Gell, D. A., et al. (2009). Analysis of Titan's neutral upper atmosphere from Cassini ion neutral mass spectrometer measurements. *Icarus*, *200*(2), 581–615. https://doi.org/10.1016/j.icarus.2008.12.005
Dartois, E., Muñoz Caro, G. M., Deboffle, D., & d'Hendecourt, L. (2004). Diffuse interstellar medium organic polymers: Photoproduction of the 3.4, 6.85 and 7.25 $\boldmath {\mu}$m features. *Astronomy & Astrophysics*, *423*(3), L33–L36. https://doi.org/10.1051/0004-6361:200400032
Dawes, A., Pascual, N., Hoffmann, S. V., Jones, N. C., & Mason, N. J. (2017). Vacuum ultraviolet photoabsorption spectroscopy of crystalline and amorphous benzene. *Physical Chemistry Chemical Physics*, *19*(40), 27544–27555. https://doi.org/10.1039/C7CP05319C
De Kok, R., Irwin, P., Teanby, N., Nixon, C., Jennings, D., Fletcher, L., et al. (2007). Characteristics of Titan's stratospheric aerosols and condensate clouds from Cassini CIRS far-infrared spectra. *Icarus*, *191*(1), 223–235. https://doi.org/10.1016/j.icarus.2007.04.003
Delitsky, M. L., & McKay, C. P. (2010). The photochemical products of benzene in Titan's upper atmosphere. *Icarus*, *207*(1), 477–484. https://doi.org/10.1016/j.icarus.2009.11.002
Fraser, H. J., Collings, M. P., McCoustra, M. R. S., & Williams, D. A. (2001). Thermal desorption of water ice in the interstellar medium. *Monthly Notices of the Royal Astronomical Society*, *327*(4), 1165–1172.
Fulchignoni, M., Ferri, F., Angrilli, F., Ball, A. J., & others (2005). In situ measurements of the physical characteristics of Titan's environment. *Nature*, *438*(7069), 785.
Gautier, T., Sebree, J. A., Li, X., Pinnick, V. T., Grubisic, A., Loeffler, M. J., et al. (2017). Influence of trace aromatics on the chemical growth mechanisms of Titan aerosol analogues. *Planetary and Space Science*, *140*, 27–34. https://doi.org/10.1016/j.pss.2017.03.012
Ghanem, A., Bokobza, L., Noel, C., & Marchon, B. (1987). Conformational analysis of p-terphenyl by vibrational spectroscopy. *Journal of Molecular Structure*, *159*(1), 47–63. https://doi.org/10.1016/0022-2860(87)85006-8
Griffith, C. A., Penteado, P., Rannou, P., Brown, R., Boudon, V., Baines, K. H., et al. (2006). Evidence for a Polar Etahne Cloud on Titan. *Science*, *313*(5793), 1620–1622.
Griffith, D. W. T., Kent, J. E., & O'Dwyer, M. F. (1975). The vibrational spectra of Dewar benzene and benzvalene. *Australian Journal of Chemistry*, *28*(7), 1397–1416. https://doi.org/10.1071/ch9751397
Gudipati, M. S., Jacovi, R., Couturier-Tamburelli, I., Lignell, A., & Allen, M. (2013). Photochemical activity of Titan's low-altitude condensed haze. *Nature Communications*, *4*, 1648. https://doi.org/10.1038/ncomms2649
Halford, R. S., & Schaeffer, O. A. (1946). Motions of Molecules in Condensed Systems. II. The Infra-Red Spectra for Benzene Solid, Liquid, and Vapor in the Range from 3 to 16.7 μ. *The Journal of Chemical Physics*, *14*(3), 141–149. https://doi.org/10.1063/1.1724114
Hanel, R., Conrath, B., Flasar, F. M., Kunde, V., Maguire, W., Pearl, J., et al. (1981). Infrared Observations of the Saturnian System from Voyager 1. *Science*, *212*(4491), 192–200. https://doi.org/10.1126/science.212.4491.192
Herzberg, G. (1945). *Molecular spectra and molecular structure. Vol. 2: Infrared and Raman spectra of polyatomic molecules. Molecular spectra and molecular structure. Vol.2: Infrared and Raman spectra of polyatomic molecules, by G. Herzberg*. New York: Van Nostrand. http://adsabs.harvard.edu/abs/1945msms.book
Hollenberg, J. L., & Dows, D. A. (1962). Absolute infrared intensities in crystalline benzene. *The Journal of Chemical Physics*, *37*(6), 1300–1307. https://doi.org/10.1063/1.1733278
Hörst, S. M. (2017). Titan's atmosphere and climate. *Journal of Geophysical Research: Planets*, *122*(3), 432–482. https://doi.org/10.1002/2016JE005240
Imanaka, H., Khare, B. N., Elsila, J. E., Bakes, E. L. O., McKay, C. P., Cruikshank, D. P., et al. (2004). Laboratory experiments of Titan tholin formed in cold plasma at various pressures: Implications for nitrogen-containing polycyclic aromatic compounds in Titan haze. *Icarus*, *168*(2), 344–366. https://doi.org/10.1016/j.icarus.2003.12.014
Ishii, K., Nakayama, H., Yoshida, T., Usui, H., & Koyama, K. (1996). Amorphous State of Vacuum-Deposited Benzene and Its Crystallization. *Bulletin of the Chemical Society of Japan*, *69*(10), 2831–2838. https://doi.org/10.1246/bcsj.69.2831
Johnstone, D. E., & Sodeau, J. R. (1991). Matrix-controlled photochemistry of benzene and pyridine. *Journal of Physical Chemistry*, *95*(1), 165–169. https://doi.org/10.1021/j100154a033
Khanna, R. K., Perera-Jarmer, M. A., & Ospina, M. J. (1987). Vibrational infrared and Raman spectra of diacyanoacetylene. *Spectrochimica Acta Part A: Molecular Spectroscopy*, *43*(3), 421–425.
Kim, S. J., Jung, A., Sim, C. K., Courtin, R., Bellucci, A., Sicardy, B., et al. (2011). Retrieval and tentative indentification of the 3μm spectral feature in Titan's haze. *Planetary and Space Science*, *59*(8), 699–704. https://doi.org/10.1016/j.pss.2011.02.002
Koehler, B. G. (2001). Desorption kinetics of model polar stratospheric cloud films measured using Fourier Transform Infrared Spectroscopy and Temperature-Programmed Desorption. *International Journal of Chemical Kinetics*, *33*(5), 295–309.
Koskinen, T. T., Yelle, R. V., Snowden, D. S., Lavvas, P., Sandel, B. R., Capalbo, F. J., et al. (2011). The mesosphere and lower thermosphere of Titan revealed by Cassini/UVIS stellar occultations. *Icarus*, *216*(2), 507–534. https://doi.org/10.1016/j.icarus.2011.09.022
Krasnopolsky, V. A. (2014). Chemical composition of Titan's atmosphere and ionosphere: Observations and the photochemical model. *Icarus*, *236*, 83–91. https://doi.org/10.1016/j.icarus.2014.03.041
Kunde, V. G., Aikin, A. C., Hanel, R. A., Jennings, D. E., Maguire, W. C., & Samuelson, R. E. (1981). C4H2, HC3N and C2N2 in Titan's atmosphere. *Nature*, *292*(5825), 686–688. https://doi.org/10.1038/292686a0
Larkin, P. (2011). *Introduction. Infrared and Raman Spectroscopy : Principles and spectral interpretation*. Elsevier. https://doi.org/10.1016/B978-0-12-386984-5.10001-1
Lavvas, P. P., Coustenis, A., & Vardavas, I. M. (2008). Coupling photochemistry with haze formation in Titan's atmosphere, Part II: Results and validation with Cassini/Huygens data. *Planetary and Space Science*, *56*(1), 67–99. https://doi.org/10.1016/j.pss.2007.05.027
Lavvas, P., Griffith, C. A., & Yelle, R. V. (2011). Condensation in Titan's atmosphere at the Huygens landing site. *Icarus*, *215*(2), 732–750. https://doi.org/10.1016/j.icarus.2011.06.040
Lavvas, P., Yelle, R. V., & Griffith, C. A. (2010). Titan's vertical aerosol structure at the Huygens landing site: Constraints on particle size, density, charge, and refractive index. *Icarus*, *210*(2), 832–842. https://doi.org/10.1016/j.icarus.2010.07.025
Lavvas, P., Yelle, R. V., Koskinen, T., Bazin, A., Vuitton, V., Vigren, E., et al. (2013). Aerosol growth in Titan's ionosphere. *Proceedings of the National Academy of Sciences*, *110*(8), 2729–2734. https://doi.org/10.1073/pnas.1217059110
Lebonnois, S. (2002). Transition from Gaseous Compounds to Aerosols in Titan's Atmosphere. *Icarus*, *159*(2), 505–517. https://doi.org/10.1006/icar.2002.6943
Lebonnois, S. (2005). Benzene and aerosol production in Titan and Jupiter's atmospheres: a sensitivity study. *Planetary and Space Science*, *53*(5), 486–497. https://doi.org/10.1016/j.pss.2004.11.004

Liang, M.-C., Yung, Y. L., & Shemansky, D. E. (2007). Photolytically generated aerosols in the mesosphere and thermosphere of Titan. *The Astrophysical Journal*, *661*(2), L199–L202. https://doi.org/10.1086/518785

Loison, J. C., Dobrijevic, M., & Hickson, K. M. (2019). The photochemical production of aromatics in the atmosphere of Titan. *Icarus*, *329*, 55–71. https://doi.org/10.1016/j.icarus.2019.03.024

Mahjoub, A., Schwell, M., Carrasco, N., Benilan, Y., Cernogora, G., Szopa, C., & Gazeau, M.-C. (2016). Characterization of aromaticity in analogues of titan's atmospheric aerosols with two-step laser desorption ionization mass spectrometry. *Planetary and Space Science*, *131*, 1–13. https://doi.org/10.1016/j.pss.2016.05.003

Mair, R. D., & Hornig, D. F. (1949). The Vibrational Spectra of Molecules and Complex Ions in Crystals. II. Benzene. *The Journal of Chemical Physics*, *17*(12), 1236–1247. https://doi.org/10.1063/1.1747149

Mayo, L., & Samuelson, R. (2005). Condensate clouds in Titan's north polar stratosphere. *Icarus*, *176*(2), 316–330. https://doi.org/10.1016/j.icarus.2005.01.020

Nakashima, N., & Yoshihara, K. (1982). Laser flash photolysis of Benzene. IV. Physicochemical properties of mist produced by laser excitation. *Bulletin of the Chemical Society of Japan*, *55*(9), 2783–2787. https://doi.org/10.1246/bcsj.55.2783

Nixon, C. A., Jennings, D. E., Bézard, B., Vinatier, S., Teanby, N. A., Sung, K., et al. (2013). Detection of propene in Titan's stratosphere. *The Astrophysical Journal*, *776*, L14. https://doi.org/10.1088/2041-8205/776/1/L14

Palmer, M. Y., Cordiner, M. A., Nixon, C. A., Charnley, S. B., Teanby, N. A., Kisiel, Z., et al. (2017). ALMA detection and astrobiological potential of vinyl cyanide on Titan. *Science Advances*, *3*(7), e1700022. https://doi.org/10.1126/sciadv.1700022

Pantos, E., Philis, J., & Bolovinos, A. (1978). The extinction coefficient of benzene vapor in the region 4.6 to 36 eV. *Journal of Molecular Spectroscopy*, *72*(1), 36–43. https://doi.org/10.1016/0022-2852(78)90041-3

Quirico, E., Montagnac, G., Lees, V., McMillan, P. F., Szopa, C., Cernogora, G., et al. (2008). New experimental constraints on the composition and structure of tholins. *Icarus*, *198*(1), 218–231. https://doi.org/10.1016/j.icarus.2008.07.012

Rahul, K. K., Shivakarthik, E., Meka, J. K., Das, A., Chandrasekaran, V., Rajasekhar, B. N., et al. (2020). Residue from vacuum ultraviolet irradiation of benzene ices: Insights into the physical structure of astrophysical dust. *Spectrochimica Acta Part A: Molecular and Biomolecular Spectroscopy*, *231*, 117797. https://doi.org/10.1016/j.saa.2019.117797

Ruiterkamp, R., Peeters, Z., Moore, M. H., Hudson, R. L., & Ehrenfreund, P. (2005). A quantitative study of proton irradiation and UV photolysis of benzene in interstellar environments. *Astronomy & Astrophysics*, *440*(1), 391–402. https://doi.org/10.1051/0004-6361:20042090

Samuelson, R. E., & Mayo, A. L. (1991). Thermal infrared properties of Titan's spectroscopic aerosol. *Icarus*, *91*(2), 207–219.

Samuelson, R. E., Mayo, L. A., Knuckles, M. A., & Khanna, R. J. (1997). C4N2 ice in Titan's north polar stratosphere. *Planetary and Space Science*, *45*(8), 941–948.

Samuelson, R. E., Smith, M. D., Achterberg, R. K., & Pearl, J. C. (2007). Cassini CIRS update on stratospheric ices at Titan's winter pole. *Icarus*, *189*(1), 63–71.

Sciamma-O'Brien, E., Ricketts, C. L., & Salama, F. (2014). The Titan Haze Simulation experiment on COSmIC: Probing Titan's atmospheric chemistry at low temperature. *Icarus*, *243*(Suppl. C), 325–336. https://doi.org/10.1016/j.icarus.2014.08.004

Sciamma-O'Brien, E., Upton, K. T., & Salama, F. (2017a). The Titan Haze Simulation (THS) experiment on COSmIC. Part II. Ex-situ analysis of aerosols produced at low temperature. *Icarus*, *289*, 214–226. https://doi.org/10.1016/j.icarus.2017.02.004

Sebree, J. A., Trainer, M. G., Loeffler, M. J., & Anderson, C. M. (2014). Titan aerosol analog absorption features produced from aromatics in the far infrared. *Icarus*, *236*, 146–152. https://doi.org/10.1016/j.icarus.2014.03.039

Strazzulla, G., & Baratta, G. A. (1991). Laboratory study of the IR spectrum of ion-irradiated frozen benzene. *Astronomy and Astrophysics*, *241*, 310–316.

Suto, M., Wang, X., Shan, J., & Lee, L. C. (1992). Quantitative photoabsorption and fluorescence spectroscopy of benzene, naphthalene, and some derivatives at 106–295 nm. *Journal of Quantitative Spectroscopy and Radiative Transfer*, *48*(1), 79–89. https://doi.org/10.1016/0022-4073(92)90008-R

Swenson, C. A., Person, W. B., Dows, D. A., & Hexter, R. M. (1959). Infrared Studies of Crystal Benzene. I. The Resolution and Assignment of v20 and the Relative Magnitudes of Crystal Fields in Benzene. *The Journal of Chemical Physics*, *31*(5), 1324–1328. https://doi.org/10.1063/1.1730593

Teanby, N. A., Irwin, P. G., Nixon, C. A., de Kok, R., Vinatier, S., Coustenis, A., et al. (2012). Active upper-atmosphere chemistry and dynamics from polar circulation reversal on Titan. *Nature*, *491*(7426), 732–735.

Toh, S. Y., Djuricanin, P., Momose, T., & Miyazaki, J. (2015). UV photochemistry of benzene and cyclohexadienyl radical in solid parahydrogen. *The Journal of Physical Chemistry A*, *119*(11), 2683–2691. https://doi.org/10.1021/jp5098537

Toumi, A., Piétri, N., Chiavassa, T., & Couturier-Tamburelli, I. (2016). Acrylonitrile characterization and high energetic photochemistry at Titan temperatures. *Icarus*, *270*, 435–442. https://doi.org/10.1016/j.icarus.2014.10.042

Trainer, M. G., Sebree, J. A., Yoon, Y. H., & Tolbert, M. A. (2013). The influence of benzene as a trace reactant in titan aerosol analogs. *The Astrophysical Journal Letters*, *766*(1), L4. https://doi.org/10.1088/2041-8205/766/1/L4

Varakin, V. N. (2018). Photolysis of adsorbed benzene at 248 nm. *Journal of Photochemistry and Photobiology A: Chemistry*, *356*, 298–303. https://doi.org/10.1016/j.jphotochem.2017.12.045

Vasconcelos, F. A., Pilling, S., Agnihotri, A., Rothard, H., & Boduch, P. (2020). Methylenimine and cyanomethanimine synthesis from ion irradiation of N2-CH4 ice: Implication on the formation of prebiotic molecules in outer solar system bodies. *Icarus*, *351*, 113944.

Vinatier, S., Bézard, B., Lebonnois, S., Teanby, N. A., Achterberg, R. K., Gorius, N., et al. (2015). Seasonal variations in Titan's middle atmosphere during the northern spring derived from Cassini/CIRS observations. *Icarus*, *250*, 95–115. https://doi.org/10.1016/j.icarus.2014.11.019

Vinatier, S., Bézard, B., Nixon, C. A., Mamoutkine, A., Carlson, R. C., Jennings, D. E., et al. (2010). Analysis of Cassini/CIRS limb spectra of Titan acquired during the nominal mission. *Icarus*, *205*(2), 559–570. https://doi.org/10.1016/j.icarus.2009.08.013

Vinatier, S., Schmitt, B., Bezard, B., Rannou, P., Dauphin, C., de Kok, R., et al. (2018). Study of Titan's fall southern stratospheric polar cloud composition with Cassini/CIRS: Detection of benzene ice. *Icarus*, *310*, 89–104.

Vuitton, V., Doussin, J.-F., Bénilan, Y., Raulin, F., & Gazeau, M.-C. (2006). Experimental and theoretical study of hydrocarbon photochemistry applied to Titan stratosphere. *Icarus*, *185*(1), 287–300. https://doi.org/10.1016/j.icarus.2006.06.002

Vuitton, V., Yelle, R. V., & Cui, J. (2008). Formation and distribution of benzene on Titan. *Journal of Geophysical Research*, *113*(E5), E05007. https://doi.org/10.1029/2007JE002997

Waite, J. H., Niemann, H., Yelle, R. V., Kasprzak, W. T., Cravens, T. E., Luhmann, J. G., et al. (2005). Ion neutral mass spectrometer results from the first flyby of Titan. *Science*, *308*(5724), 982–986.

Waite, J. H., Young, D. T., Cravens, T. E., Coates, A. J., Crary, F. J., Magee, B., & Westlake, J. (2007). The Process of tholin formation in Titan's upper atmosphere. *Science*, *316*(5826), 870–875. https://doi.org/10.1126/science.1139727

Wheeless, C. J. M., Zhou, X., & Liu, R. (1995). Density functional theory study of vibrational spectra. 2. Assignment of fundamental vibrational frequencies of fulvene. *Journal of Physical Chemistry*, *99*(33), 12488–12492. https://doi.org/10.1021/j100033a019

Wilson, E. H. (2004). Current state of modeling the photochemistry of Titan's mutually dependent atmosphere and ionosphere. *Journal of Geophysical Research*, *109*(E6), E06002. https://doi.org/10.1029/2003JE002181

Wilson, E. H., & Atreya, S. K. (2003). Chemical sources of haze formation in Titan's atmosphere. *Planetary and Space Science*, *51*(14–15), 1017–1033. https://doi.org/10.1016/j.pss.2003.06.003

Wilson, E. H., & Atreya, S. K. (2004). Current state of modeling the photochemistry of Titan's mutually dependent atmosphere and ionosphere. *Journal of Geophysical Research*, *109*(E6), E06002. https://doi.org/10.1029/2003JE002181

Yokoyama, A., Zhao, X., Hintsa, E. J., Continetti, R. E., & Lee, Y. T. (1990). Molecular beam studies of the photodissociation of benzene at 193 and 248 nm. *The Journal of Chemical Physics*, *92*(7), 4222–4233. https://doi.org/10.1063/1.457780

Yoon, Y. H., Hörst, S. M., Hicks, R. K., Li, R., de Gouw, J. A., & Tolbert, M. A. (2014). The role of benzene photolysis in Titan haze formation. *Icarus*, *233*(Suppl C), 233–241. https://doi.org/10.1016/j.icarus.2014.02.006

Yung, Y. L., Allen, M., & Pinto, J. P. (1984). Photochemistry of the atmosphere of Titan-Comparison between model and observations. *The Astrophysical Journal Supplement Series*, *55*, 465–506.

Zhou, X., & Liu, R. (1997). Density functional theory study of vibrational spectra, 6: assignment of fundamental vibrational frequencies of benzene isomers: Dewar benzene, benzvalene, trimethylenecyclopropane, prismane, and 3,4-dimethylenecyclobutene. *Spectrochimica Acta Part A: Molecular and Biomolecular Spectroscopy*, *53*(2), 259–269. https://doi.org/10.1016/S1386-1425(96)01724-6